Chinese Chemical Letters 32 (2021) 2400–2404

Contents lists available at ScienceDirect

Chinese Chemical Letters

journal homepage: www.elsevier.com/locate/cclet

Communication

# Tirapazamine encapsulated hyaluronic acid nanomicelles realized targeted and efficient photo-bioreductive cascading cancer therapy

Chunhui Wu[a,*], Qiuyue Liu[a], Yikun Wang[a], Zhengxin Xie[a], Honglin Huang[a], Ningxi Li[a], Xiaodan Wei[a], Geng Yang[a], Tingting Li[a], Hong Yang[a], Shun Li[a], Xiang Qin[a], Yiyao Liu[a,b,*]

[a] Department of Biophysics, School of Life Science and Technology, University of Electronic Science and Technology of China, Chengdu 610054, China
[b] TCM Regulating Metabolic Diseases Key Laboratory of Sichuan Province, Hospital of Chengdu University of Traditional Chinese Medicine, Chengdu 610072, China

ARTICLE INFO

*Article history:*
Received 6 January 2021
Received in revised form 24 February 2021
Accepted 25 February 2021
Available online 27 February 2021

*Keywords:*
Hyaluronic acid
Photosensitizer
Bioreductive prodrug
Hypoxia
Cascading cancer therapy

ABSTRACT

Currently, architecting a rational and efficient nanoplatform combing with multi-therapeutic modalities is highly obligatory for advanced cancer treatment. In order to remedy the self-limiting hypoxic dilemma of photodynamic therapy (PDT), herein, a facile photosensitizer (*i.e.*, chlorin e6, Ce6) and bioreductive prodrug (*i.e.*, tirapazamine, TPZ)-coloaded hyaluronic acid (HA) nanomicelles (denoted as TPZ@HA-Ce6) was developed for the cascading mode of photo-bioreductive cancer therapy. Taking the typical advantage of Ce6 coupled HA conjugate, TPZ was easily and successfully accommodated into the hydrophobic core of HA-Ce6 nanomicelles, yielding TPZ@HA-Ce6. It showed good dispersibility and stability with the hydrodynamic size of *ca.* 170 nm. It targeted the CD44 overexpressed cancer cells by receptor-mediated endocytosis way and killed them effectively with singlet oxygen and the subsequent TPZ radicals resulting from the oxygen depletion of PDT. The later was further verified by the hypoxia probe *in vivo*. Using murine mammary carcinoma 4T1 model, TPZ@HA-Ce6 nanomicelles exhibited cascading and synergistic anticancer effect of PDT and TPZ bioreductive therapy compared with each monotherapy. This work suggests the promising prospect of the hybrid hyaluronic nanomicelles for highly efficient cancer combination treatment.



Cancer still challenges human being's life and health in the world. Though many therapeutic techniques are applied in clinics, any single one could not successfully conquer the malignant tumor due to its limited efficiency. Currently, developing the advanced therapeutic approach against cancer is being attached enormous attention, which is usually architected on a nanoplatform combining with two or three therapeutic modalities for the maximum therapeutic efficacy with minimal side effects [1]. As a typical and traditional therapeutic technique based on the reactive oxygen species (ROS), PDT is still received tremendous attention due to its effectiveness, selectivity, noninvasiveness, controllability and *etc.* [2,3]. From the main principle of PDT (type II), *i.e.* photochemical reaction of photosensitizers with oxygen upon laser irradiation, the ROS yield is greatly dependent on the concentration of oxygen [4]. However, one common microenvironment hallmark of solid tumor is hypoxia, which is caused by the abnormal vasculature and the chaotic tumor blood flow and gets serious from outside to the inside of tumor, thus greatly diminishing the efficiency of PDT [5]. Also, with PDT proceeds, the intratumoral oxygen would be gradually consumed, and this self-limiting effect further decreases the photokilling effect [5]. Even worse, the induced hypoxia state after PDT could increase the metastatic potency of tumors by stimulating the release of hypoxia inducible factor $1\alpha$ (HIF-$1\alpha$) and vascular endothelial growth factor at the tumor-stromal interface [6].

Mounting strategies have been conceived to combat the hypoxic dilemma post-PDT, like the hyperoxygenation treatment [7], using nanoenzyme (*e.g.*, $MnO_2$) to yield oxygen [8], or combining with the inhibitor of HIF-$1\alpha$ [9], thus enhancing the tumoricidal efficiency of PDT. Among of which, combination with the hypoxia-activated prodrug with photosensitizer provides an effective way to further eliminate the remaining cancer cells with the produced highly cytotoxic agents [10,11]. As one typical reductive prodrug, tirapazamine (TPZ) could generate the free-radical intermediate cytotoxic species (*i.e.*, hydroxyl radical and

* Corresponding authors at: Department of Biophysics, School of Life Science and Technology, University of Electronic Science and Technology of China, Chengdu 610054, China.
*E-mail addresses:* wuchunhui@uestc.edu.cn (C. Wu), liuyiyao@uestc.edu.cn (Y. Liu).

https://doi.org/10.1016/j.cclet.2021.02.060

benzotriazinyl radical) under low-oxygen conditions and remove the hydrogen atoms from the nearby macromolecules to cause the structural damages [12]. TPZ had been encapsulated into various inorganic and organic nanosystems for cancer combination therapy [12–18]. For example, Gu's group had designed a ROS responsive nanovesicle to release the loaded TPZ for further enhanced cell apoptosis [14]. Furthermore, an angiogenic vessel targeted delivery system with capabilities of photoactively releasing TPZ achieved the amplified antitumor effect both *in vitro* and *in vivo* [15]. In order to kill the tumor cells both proximal and distal to vessels, tumor homing and penetrating peptides (*e.g.*, iRGD and TAT) were modified on the surface of photosensitizer and TPZ coloaded nanovehicles, and they significantly penetrated into the hypoxic area to eliminate all cancer cells [16,18]. Such systems were reported to be very effective, however, several problems like the relative complex preparation process, the vector-induced toxicity and the premature release of drugs, *vice versa* restrict their further development and application. Therefore, exploring a simple and effective system to deliver both photosensitizer and TPZ into the tumor for the highly efficient therapeutic outcome is very desirable.

Hyaluronic acid (HA) is a well-known excellent and widely applied natural polymer in biomedical and pharmaceutical areas [19]. As a kind of glycosaminoglycan component of the extracellular matrix, HA with a backbone of alternating D-glucuronic acid and *N*-acetyl-D-glucosamine units is hydrophilic, biodegradable, biocompatible and immunoneutral. Especially, it could target the receptors such as CD44 overexpressed on many kinds of tumor cells' surface [20,21]. So HA has been extensively utilized to functionalize the nanovehicles to confer the stability, compatibility and targeting ability [22–24]. Another way, many hydrophobic molecules were linked to HA to yield the amphiphilic conjugate [22–27], which can be self-assembled into nanomicelles under aqueous conditions. Moreover, these nanomicelles could harbor other anticancer drugs and/or imaging probes into their hydrophobic inner cores for cancer theranostics [20,25,26]. Also, these systems could be digested by hyaluronidase (HAase) overexpressed in tumor cells and exhibit enzyme stimulated "On/Off" releasing behavior of its cargoes [21,27]. Particularly, photosensitizers had been integrated into the HA based nanosystems to realize multimode imaging (*e.g.*, fluoresce imaging, photoacoustic imaging) guided tumor photoablation both *in vitro* and *in vivo* [27–29]. In a word, HA provides a very mature candidate for constructing the simple and smart nanoplatform for cancer theranostics.

Based on the above, herein, we aimed to fabricate a simple photosensitizer and TPZ co-encapsulated hyaluronic acid nanomicelles for the targeted photo-bioreductive cascading treatment of cancer (Scheme 1). The clinical used photosensitizer Ce6 was chemically attached to HA to yield an amphiphilic conjugate, which formed self-assembled HA-Ce6 nanomicelles. Then, TPZ was readily loaded into the HA-Ce6 nanomicelles by ultrasonication, forming TPZ@HA-Ce6 (Scheme 1A). The detail characterization, cellular endocytosis, the photoactive properties, the intratumor hypoxic microenvironment, the synergistic anticancer activity of PDT and TPZ radials mediated chemotherapy were evaluated against 4T1 murine mammary cancer model. This work suggests a very simple but highly efficient agent of drug loaded HA nanomicelles for the combined oncotherapy.

The photo-bioreductive nanomicelles TPZ@HA-Ce6 were fabricated by two steps. Firstly, the amphiphilic HA-Ce6 conjugate was synthesized according to the reported method [27] and characterized by $^1$H NMR, UV–vis absorption and fluorescence spectroscopy (Figs. S1A–D in Supporting information). The obtained HA-Ce6 could be easily self-assembled into micelles as detected by dynamic light scattering (DLS) with the hydrodynamic diameter

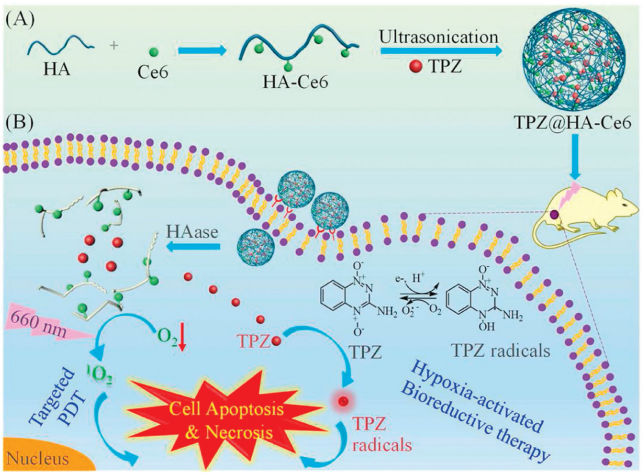


**Scheme 1.** (A) The preparation of photo-bioreductive drug loaded nanomicelles TPZ@HA-Ce6; (B) The cascading oncotherapeutic mode mediated by TPZ@HA-Ce6 nanomicelles.

*ca.* 173 nm (PDI = 0.265) and transmission electronic microscopy (TEM) (Figs. S1E and F in Supporting information). Secondly, the hydrophobic TPZ molecules were readily loaded into the HA-Ce6 nanomicelles under sonication to yield the drug loaded nanomicelles (denoted as TPZ@HA-Ce6). As shown in the UV–vis absorption spectra of TPZ@HA-Ce6 (Fig. 1A), the obvious peak at about 480 nm for TPZ and the peaks at 404 nm and 660 nm for Ce6 were clearly observed. The maximum drug loading efficacy was approximately 21% when the ratio of [Ce6]/[TPZ] = 1:0.5, and the encapsulation rate was approximately 60.0%. Measured by DLS (Fig. 1B), its hydrodynamic diameter was about 170 nm with PDI = 0.272, which was nearly the same as that of HA-Ce6 nanomicelles. Furthermore, the TEM morphically characterization showed the very well spherical shape of TPZ@HA-Ce6 with the dehydrated diameter about 100 nm (inset of Fig. 1B).

The obtained TPZ@HA-Ce6 nanomicelles could be stable in PBS as long as 96 h, as the mean hydrodynamic size kept almost unchanged (Fig. 1C). Since HA was HAase responsive, it could be observed that TPZ@HA-Ce6 partially decomposed upon interacted with HAase (Type I) for 12 h (Fig. S1G in Supporting information), indicating that TPZ and Ce6 could be released once entered cells. The photosensitive behavior of TPZ@HA-Ce6 was detected fluorescently using singlet oxygen sensor green (SOSG). With increasing the irradiation time, the singlet oxygen generation of TPZ@HA-Ce6 and HA-Ce6 increased gradually (Fig. 1D). To note, for TPZ@HA-Ce6, the singlet oxygen generation was much higher than that of HA-Ce6, indicating that TPZ may enhance the photochemical efficiency of Ce6. Meanwhile, the oxygen depletion could be detected with a dissolved oxygen meter upon laser irradiation. It could be observed that the dissolved oxygen concentration for TPZ@HA-Ce6 decreased very quickly within 30 min as compared with that of HA-Ce6 (Fig. 1E). The results were in accordance with the singlet oxygen detection. In contrast, the buffer or free TPZ itself showed no oxygen depletion under the same condition. The depletion of oxygen would result in the hypoxic environment in tumors, which triggered the activation of TPZ. Additionally, TPZ@HA-Ce6 was biocompatible and the hemolysis rate was very low (Fig. 1F).

HA was extensively demonstrated as a universal ligand recognizing the CD44 receptor, so the targeted cellular internalization of TPZ@HA-Ce6 nanomicelles was further investigated. CD44 receptor overexpressed human breast cancer cells MDA-MB-231, murine mammary cancer cells 4T1, and CD44 negative normal human breast cells MCF-10A as control were specifically chosen to

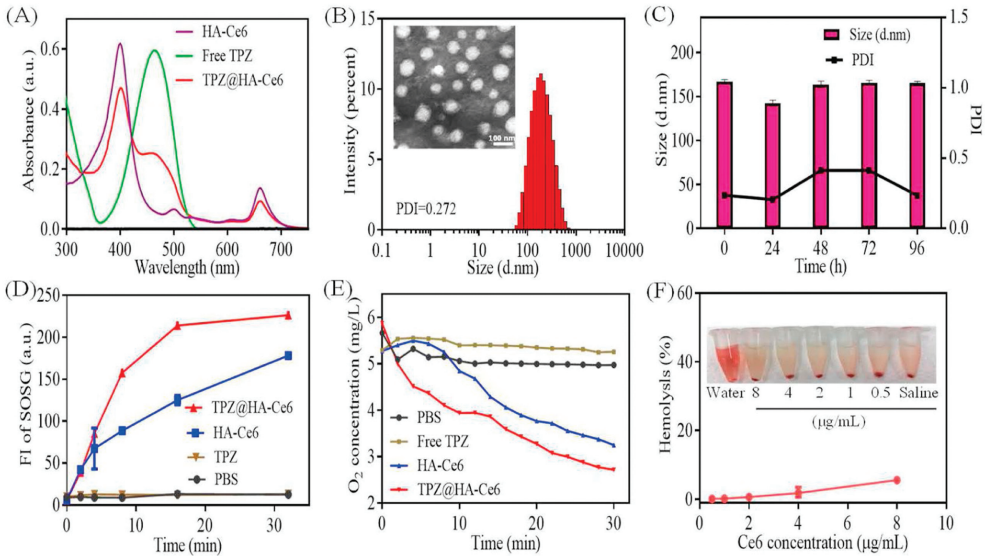


**Fig. 1.** (A) UV–vis spectroscopy, (B) DLS and TEM image (inserted) of TPZ@HA-Ce6 nanomicelles; (C) The hydrodynamic size of TPZ@HA-Ce6 nanomicelles after different standing time; (D) Singlet oxygen generation and (E) oxygen depletion profiles of TPZ@HA-Ce6 nanomicelles under irradiation; (F) Hemolysis of TPZ@HA-Ce6 nanomicelles.

be incubated with TPZ@HA-Ce6 in this work. Compared with free Ce6, TPZ@HA-Ce6 could effectively deliver Ce6 into the cancer cells (Fig. S2 in Supporting information). As shown in the confocal microscopic images in Fig. S3A (Supporting information), both the treated MDA-MB-231 and 4T1 cells exhibited significant red fluorescence signal of Ce6 in the cytoplasm after 12 h incubation, but in the treated MCF-10A cells, there were slight fluorescent signals to be observed in the cytoplasm. The results suggested that TPZ@HA-Ce6 could recognize the CD44 receptors overexpressed on the cancer cells' surfaces and then be endocytosed effectively. To further confirm this selective cellular uptake behavior, HA was incubated with the cells prior to the treatment of TPZ@HA-Ce6, and the fluorescence signals in the cytoplasm were obviously decreased (Fig. S3B in Supporting information), which mean that the cellular uptake of TPZ@HA-Ce6 was greatly inhibited by free HA. These results further demonstrated that TPZ@HA-Ce6 nanomicelles could recognize the CD44 receptor overexpressed cancer cells and then be endocytosed, thus delivering the loaded drugs into the cancer cells.

Next, we studied the *in vitro* cytotoxicity of TPZ@HA-Ce6 nanomicelles in dark. TPZ@HA-Ce6 with different ratio of [Ce6]:[TPZ] = 10:0.3, 10:1 and 10:2 were incubated with 4T1 cells for 24 h, and the relative cell viability was all above 90% at the low ratios of 10:0.3 and 10:1 except the high ratio of 10:2 (Figs. S4A–C in Supporting information and Fig. 2A), indicating that TPZ@HA-Ce6 were relatively safe to 4T1 cells in dark. TPZ@HA-Ce6 also showed negatable cytotoxicity to MCF-10A cells (Fig. S4D in Supporting information).

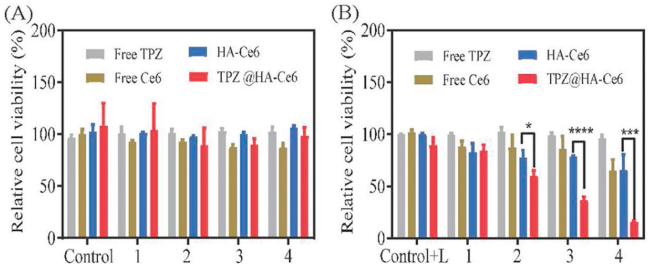


**Fig. 2.** The relative cell viability of 4T1 cancer cells treated with free Ce6, free TPZ, HA-Ce6 and TPZ@HA-Ce6 nanomicelles (A) in dark and (B) under irradiation (660 nm, 0.5 W/cm$^2$, 5 min); the concentration of Ce6 for group 1 to 4 is 1.25, 2.5, 5.0 and 10.0 μg/mL respectively; the concentration of TPZ for group 1 to 4 is 0.13, 0.25, 0.5 and 1.0 μg/mL respectively.

The photo-bioreductive cascading therapeutic efficiency of TPZ@HA-Ce6 nanomicelles was then explored against 4T1 cancer cells upon laser irradiation. Series concentration of TPZ@HA-Ce6 together with free TPZ, free Ce6 and HA-Ce6 were incubated with 4T1 cells for 12 h and then irradiated with laser (660 nm, 0.5 W/cm$^2$, 5 min), and the relative cell viability was shown in Fig. 2B. Free TPZ showed almost no anticancer activity against 4T1 cells, and HA-Ce6 showed higher photokilling efficiency than free Ce6, suggesting the targeted photodynamic anticancer activity of HA-Ce6 nanomicelles. In comparison with HA-Ce6 or free TPZ, prominent anticancer effect was observed for TPZ@HA-Ce6 treated 4T1 cancer cells upon irradiation. Moreover, TPZ@HA-Ce6 exhibited dose-dependent anticancer efficiency. For example, the relative cell viability of TPZ@HA-Ce6 + Laser (at the equiv. [Ce6] = 10.0 μg/mL and [TPZ] = 1.0 μg/mL) treated group decreased to about 16.2%, while the group treated with HA-Ce6 + Laser decreased to 65.8% at the same concentration (Fig. 2B). Such enhanced anticancer efficiencies were most probably attributed to the oxygen consumption of HA-Ce6 upon irradiation and the activated TPZ by the generated redox environment. This rational was further demonstrated by the obvious enhanced anticancer activity of TPZ@HA-Ce6 in the oxygen-deficient cell model (Fig. S5A in Supporting information) using $CoCl_2$ as a hypoxia inducer, which could directly replace $Fe^{2+}$ in heme-like substances to destroy the combinability with oxygen and/or even the oxygen-carrying activity [30,31]. TPZ@HA-Ce6 exerted much higher hypoxic environment to generate TPZ radicals than that of Ce6. To note, the cancer cell photo-killing efficiency of TPZ@HA-Ce6 was much greater than that of the mixture of free TPZ and free Ce6 (Fig. S5B in Supporting information), which further demonstrated the targeted and highly efficient cascading anticancer activity of photo-bioreductive therapy mediated by TPZ@HA-Ce6 nanomicelles.

To evaluate the *in vivo* photo-bioreductive cascading anticancer efficiency of TPZ@HA-Ce6 nanomicelles, BALB/c mice bearing 4T1 tumors were treated with saline, free TPZ, HA-Ce6 + Laser,

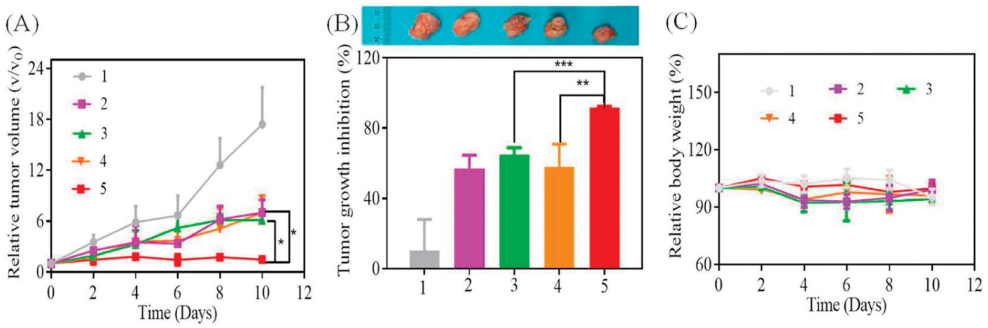


**Fig. 3.** (A) Tumor growth curves, (B) tumor inhibition rate and representative images, and (C) body weight changes of 4T1 tumor-bearing mice treated with saline (1), free TPZ (2), HA-Ce6 + Laser (3), TPZ@HA-Ce6 (4) and TPZ@HA-Ce6 + Laser (5); Significant differences were analyzed using Student's *t*-test: $^{*}P < 0.05$, $^{**}P < 0.01$, $^{***}P < 0.001$.

TPZ@HA-Ce6, TPZ@HA-Ce6 + Laser, respectively. All the procedures were approved by the Institutional Animal Care and Use Committee of University of Electronic Science and Technology of China. 6 h later, the irradiation groups were treated with 660 nm laser (1.0 W/cm$^2$, 10 min). The tumor growth rate of each group was monitored by evaluating the tumor volume for ten days (Fig. 3A). Compared with the control group, the tumor size of groups treated by free TPZ and TPZ@HA-Ce6 were moderately inhibited, which were probably due to the intrinsic hypoxic microenvironment of tumors that induce TPZ reduction. For the case of TPZ@HA-Ce6 + Laser treated group, all the tumors almost no increase during the whole experiment process, while HA-Ce6 + Laser still showed moderate inhibition efficiency. It was very clear that the combination therapy mediated by TPZ@HA-Ce6 under irradiation exerted the highest anticancer activity compared with the monotherapy. And that was because of the cascading effect of PDT mediated by HA-Ce6 and the photo-killing efficiency of TPZ radicals. At the endpoint, the tumors were taken out and the representative digital photographs of tumors showed that the tumor sizes for the TPZ@HA-Ce6 + Laser group was the smallest in all groups (Fig. 3B). The relative tumor inhibition rate was calculated to be 57.2%, 64.9%, 58.2% and 91.8% for free TPZ, HA-Ce6 + Laser, TPZ@HA-Ce6 and TPZ@HA-Ce6 + Laser group, respectively (Fig. 3B). The additive tumor inhibition rate of PDT mediated by HA-Ce6 + Laser and TPZ bioreductive therapy could be estimated (about 85.3%) according to the Formula S1 (Supporting information). TPZ@HA-Ce6 together with laser irradiation showed higher tumor inhibition rate than the additive value, suggesting again the cascading and synergistic anticancer activity of PDT and bioreduction therapy. These results were in accordance with that of the tumor volume analysis.

To reveal the rationale behind the high anticancer efficiency of TPZ@HA-Ce6 + Laser group, the extent of hypoxia in the 4T1 tumor microenvironment after treatment with TPZ@HA-Ce6+Laser was measured by pimonidazole staining, which is a well characterized exogenous hypoxia marker and bind covalently to SH-containing molecules in hypoxic tissue. It could be visualized by immunohistochemical staining following animal sacrifice. As shown in Fig. S6 (Supporting information), the green fluorescence of the tumor section for the mice treated with TPZ@HA-Ce6 was distributed throughout the whole tumor, indicating the endogenous hypoxic environment. To note, the green fluorescence signal of the hypoxic area was well colocalized with the red fluorescence signal of Ce6. The results suggested that HA-Ce6 could access the hypoxic area of tumors. For the mice treated with TPZ@HA-Ce6 + Laser, much higher fluorescence was observed, which confirmed that TPZ@HA-Ce6 plus laser augmented the existence of hypoxia in the tumors, thus it could activate TPZ for another wave of bioreductive therapeutic activity. Besides, the sufficient tumor accumulation and retention of TPZ@HA-Ce6 in tumor tissue might contribute to the enhanced therapeutic efficacy of TPZ@HA-Ce6 + Laser. During the whole experiment, the mice bodyweight of all groups was nearly no change, indicating that TPZ@HA-Ce6 was relatively safe to the mice (Fig. 3C). More discussions were in section S2 (Supporting information). Overall, this work demonstrates that TPZ@HA-Ce6 is a safe and highly effective photo-chemo agent for cancer combination therapy.

In summary, we reported a facile TPZ drug loaded nanomicelles based on the amphiphilic and biocompatible HA-photosensitizer conjugate for the cascading and synergistic photodynamic and bioreductive therapy against the malignant tumor. The obtained TPZ@HA-Ce6 nanomicelles could target the cancer cells overexpressed CD44 receptor and elicit very efficient PDT upon laser irradiation compared with free photosensitizer. The fluorescence imaging result demonstrated the induced hypoxic environment of PDT, thus activating TPZ. Against the murine mammary 4T1 cancer model, TPZ@HA-Ce6 nanomicelles could efficiently accumulated into the tumor and resulted in the excellent therapeutic efficacy due to the combined effect of photogenerated ROS and activated TPZ species. This work suggests that TPZ@HA-Ce6 could be a potent agent for highly efficient and targeted cancer combination treatment.

## Declaration of competing interest

The authors report no declarations of interest.

## Acknowledgments

This research was supported, in part or in whole, by the National Natural Science Foundation of China (Nos. 81471785, 81671821, 11772088, 11802056, 31800780, 11972111, 31900940, U19A2006, 32071304), the Basic Research Program of Sichuan Science and Technology (Nos. 2021YJ0130, 2019YJ0183, 2019YJ0184), China Postdoctoral Science Foundation (Nos. 2018M640904, 2019T120831), and the Fundamental Research Funds for the Central Universities (No. ZYGX2019J117).

## Appendix A. Supplementary data

Supplementary material related to this article can be found, in the online version, at doi:https://doi.org/10.1016/j.cclet.2021.02.060.

## References

[1] S. Rawal, M.M. Patel, J. Control. Release 301 (2019) 76–109.
[2] L.M. Yang, P. Gao, Y.L. Huang, et al., Chin. Chem. Lett. 30 (2019) 1293–1296.
[3] L. Li, Y.S. Chen, W.J. Chen, et al., Chin. Chem. Lett. 30 (2019) 1689–1703.
[4] J.P. Celli, B.Q. Spring, I. Rizvi, et al., Chem. Rev. 110 (2010) 2795–2838.

[5] X. Li, N. Kwon, T. Guo, et al., Angew Chem. Int. Ed. 57 (2018) 11522–11531.
[6] M.I. Koukourakis, A. Giatromanolaki, J. Skarlatos, et al., Cancer Res. 61 (2001) 1830–1832.
[7] Z. Huang, Q. Chen, A. Shakil, et al., Photochem. Photobiol. 78 (2003) 496–502.
[8] G. Yang, L. Xu, Y. Chao, et al., Nat. Commun. 8 (2017) 902.
[9] Z. Zhang, R. Wang, X. Huang, et al., ACS Appl. Mater. Interfaces 12 (2020) 5680–5694.
[10] W.R. Wilson, M.P. Hay, Nat. Rev. Cancer 11 (2011) 393–410.
[11] L. Feng, L. Cheng, Z. Dong, et al., ACS Nano 11 (2017) 927–937.
[12] Y. Liu, Y. Liu, W. Bu, et al., Angew Chem. Int. Ed. 54 (2015) 8105–8109.
[13] Y. Shao, B. Liu, Z. Di, et al., J. Am. Chem. Soc. 142 (2020) 3939–3946.
[14] C. Qian, P. Feng, J. Yu, et al., Angew Chem. Int. Ed. 56 (2017) 2588–2593.
[15] D. Guo, S. Xu, N. Wang, et al., Biomaterials 144 (2017) 188–198.
[16] Y. Wang, Y. Xie, J. Li, et al., ACS Nano 11 (2017) 2227–2238.
[17] D. Chen, Y. Tang, J. Zhu, et al., Biomaterials 221 (2019) 119422.
[18] K.M. Ihsanullah, B.N. Kumar, Y. Zhao, et al., Biomaterials 245 (2020) 119982.
[19] H. Kim, H. Jeong, S. Han, et al., Biomaterials 123 (2017) 155–171.
[20] P. Kesharwani, S. Banerjee, S. Padhye, et al., Biomacromolecules 16 (2015) 3042–3053.
[21] Q. Zhao, J. Liu, W. Zhu, et al., Acta Biomater. 23 (2015) 147–156.
[22] J. Han, W. Park, S.J. Park, et al., ACS Appl. Mater. Interfaces 8 (2016) 7739–7747.
[23] W. Miao, G. Shim, C.M. Kang, et al., Biomaterials 34 (2013) 9638–9647.
[24] Y. Sakurai, H. Harashima, Expert Opin. Drug Del. 16 (2019) 915–936.
[25] H.Y. Yoon, H. Koo, K.Y. Choi, et al., Biomaterials 33 (2012) 3980–3989.
[26] H.J. Cho, H.Y. Yoon, H. Koo, et al., Biomaterials 32 (2011) 7181–7190.
[27] W. Li, C. Zheng, Z. Pan, et al., Biomaterials 101 (2016) 10–19.
[28] Y. Li, L. Sutrisno, Y. Hou, et al., Chem. Commun (Camb.) 56 (2020) 9978–9981.
[29] X. Liang, L. Fang, X. Li, et al., Biomaterials 132 (2017) 72–84.
[30] F.F. Xue, W.X. Du, S.X. Chen, et al., ACS Appl. Bio Mater. 3 (2020) 8962–8969.
[31] Y. Huang, K.M. Du, Z.H. Xue, et al., Leukemia 17 (2003) 2065–2073.